Lower temperature electrochemical reduction of lunar regolith simulants in molten salts

Authors: Alexandre Meurisse*[1], Bethany Lomax[1,2], Áron Selmeci[1], Melchiorre Conti[1], Robert Lindner[1], Advenit Makaya[1], Mark D. Symes[2], James Carpenter[1]

[1] European Space Research and Technology Centre (ESTEC), Keplerlaan 1, 2201 AZ Noordwijk, The Netherlands

[2] WestCHEM, School of Chemistry, University of Glasgow, Glasgow G12 8QQ, United Kingdom

*corresponding author: alexandre.meurisse@esa.int

Abstract

Extraction of oxygen from lunar soil is key to the sustainability of human and robotic operations on the Moon and would open the path to in-space refuelling with space resources. This work investigates reducing the temperature of the electrochemical FFC process, by changing the salt from pure $CaCl_2$ to eutectic mixtures with KCl, NaCl and LiCl. Initial experimental results demonstrate the feasibility of removing at least 40% of the oxygen present in lunar minerals in 24 hours in all eutectics and at temperatures as low as 660 °C; 85% of the oxygen could be removed in the comparative experiment using the baseline conditions of $CaCl_2$ at 950 °C. Besides the expected impact on the kinetics when running the process at lower temperature, parasitic reactions linked to the graphite anode's interaction with the extracted oxygen, calcium cycling between the electrodes, and other mechanisms specific to each salt mixture appear to have a significant impact on the reduction process. Further work is needed to understand the limiting factors for the reduction in each eutectic salt electrolyte.

Introduction

Human and robotic space exploration missions beyond Low Earth Orbit have recently experienced a second wind. Numerous public institutions and private actors across the globe are targeting the Moon, and potentially Mars, for scientific and commercial activities [1]. The Moon, given its proximity to the Earth, has attracted the most interest for missions in the coming decade. The upcoming European payload PROSPECT on-board the Russian Luna 27 mission, the announcement of the CLPS (Commercial Lunar Payload Services) and Artemis programmes in the US, as well as the recent successful robotic missions of the Chinese Chang'e programme and attempts from India and Israel have pushed the world to look up to our natural satellite. Most of these missions are, however, of relatively short duration, undertaken in preparation for longer duration missions that could establish permanent outposts at the lunar surface. Such achievement in the near future will rely on technology and materials to sustain the human and robotic presence on the lunar surface, which will involve vehicle and rocket refuelling, infrastructure construction, and maintenance of life-support systems, rovers, and human lunar habitats. One approach is to utilise the resources of space.

The idea to use space resources is not novel [2], but their actual utilisation has not yet been realised and may become a crucial enabler to achieve the long-term sustainability needs of the ever increasing number of space faring nations. In-situ resource utilisation (ISRU) describes the use of space resources at the point of need to reduce mass launched from Earth and the overall mission risk. On the Moon, the lunar soil is ubiquitous and easily accessible and so it will likely be an important resource. The fine dust covering the Moon, or *regolith*, is composed of oxygen and metals bonded in complex mineral and amorphous structures. Extracting the oxygen from lunar soil (40 to 45 wt.%) could enable refuelling capabilities at the surface and potentially support life support systems, while the left-over metal elements could find application in manufacturing and construction. Over the last 20 years many chemical and electrochemical processes have been developed and tested to extract oxygen from lunar regolith simulants [3]–[10], yet only a molten salt electrolysis process, based on the Fray Farthing Chen (FFC) Cambridge process, has demonstrated a full reduction of the material [11], [12].

The FFC Cambridge process is an electrochemical process that uses molten salts as the electrolyte [13]. Based on terrestrial industrial experience, standard working parameters have been found to fully reduce lunar regolith simulants [11]. A FFC Cambridge process that uses molten $CaCl_2$ with 0.4 wt.% of CaO at 950 °C can reduce every oxide mineral constituting lunar regolith. However, running the process at such a high temperature requires a lot of power and promotes the deterioration of materials used in the electrochemical cell. Furthermore, high temperatures may also contribute to the instability of inert anodes, which are necessary for the direct production of oxygen. While replacing damaged cell parts is not a significant problem on Earth, it could become a showstopper for autonomous large-scale operations on the lunar surface. Therefore, finding the means to reduce the process temperature is relevant to decreasing the deterioration rate of the components, and opening the materials selection to new options not available at 950 °C.

Demonstration of the electrochemical reduction of oxides at lower temperature in molten salts was mainly shown with actinides (e.g. U, Pu, Am) for recycling processed nuclear fuels [14]–[18]. Other studies have shown reduction of simple oxides at temperatures between 550 - 850 ^{O}C in various electrolyte compositions [19]–[26]. Typically, processes proposed for the extraction of oxygen from lunar regolith, including molten salt electrolysis, utilise temperatures >900 ^{O}C to achieve a reasonable extraction percentage [9]. Reducing the temperature required for the extraction of lunar resources would be highly beneficial.

This paper presents an investigation into the electrochemical reduction of a lunar regolith simulant at temperatures from 660 to 950 °C using $CaCl_2$, LiCl, and $CaCl_2$-XCl (X=Li, K, Na) eutectic mixtures. The goal of this research was to understand the potential promise and challenges associated with reducing the FFC Cambridge process temperature, and their impact on the reduction of lunar minerals.

Materials and Methods

Lunar simulant

Lunar regolith is a mix of fine and coarse rock fragments, resulting from the steady micro-meteoroid bombardment occurring on the Moon for the past few billion years. This regolith material is mainly

composed of basaltic rocks in the maria, the visually darker regions that contain younger material, and anorthositic rocks in the highlands, the lighter regions that cover over 84% of the lunar surface [27]. Less than 400 kg of regolith has been returned from the Moon, most of it during the Apollo missions in the early 70s. Using this material for destructive ISRU processes is possible [28], but limited to a small quantity that is insufficient for most research works. Therefore, researchers and engineers have developed lunar simulants, which are lunar analogue materials created from processed terrestrial materials. They mimic some of the physico-chemical features of the lunar soil. This work uses LMS-1, a Lunar Mare Simulant developed by CLASS Exolith Lab from the University of Central Florida [29]. The mineralogy and bulk chemistry, and particle size distribution are given in Table 1, Table 2, and Figure 1, respectively.

Table 1: LMS-1 mineralogy [29]

Mineralogy	**LMS-1**
Component	**Wt.%**
Pyroxene	32.8
Glass-rich basalt	32.0
Anorthosite	19.8
Olivine	11.1
Ilmenite	4.3

Table 2: LMS-1 bulk chemistry [29]. The composition of a sample of Apollo 11 High-Ti Mare regolith was added for comparison [30].

Bulk chemistry	**LMS-1**	**Apollo 11 sample 10084, 1591**
Oxide	**Wt.%**	**Wt.%**
SiO_2	42.81	41.3
MgO	18.89	8.0
Al_2O_3	14.13	13.7
FeO_T^*	7.87	15.8
CaO	5.94	12.5
Na_2O	4.92	0.41
TiO_2	4.62	7.5
K_2O	0.57	0.14
P_2O_5	0.44	/
Cr_2O_3	0.21	0.290
MnO	0.15	0.213
SO_3	0.11	/
Total	100.00	99.85

*: Fe^{2+} and Fe^{3+} are not distinguished

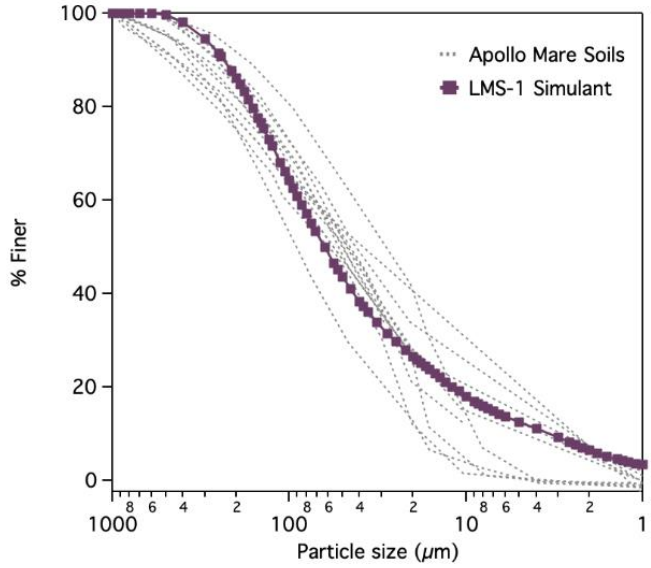

Figure 1: LMS-1 and Apollo particle size distributions [29].

Both powder and solid pellet samples can be used in the FFC Cambridge process. Powder samples are often less dense than pellets, thus allowing for a better electrolyte flow and overall better reduction. The electrolyte flow can however also displace fine powders out the cathode basket. The powder falling of the basket is left unreduced and can pollute the salt over time. Porous pellets are therefore a good alternative as they prevent the loss of material and still allow a good electrolyte flow and reduction [31]. Pellets can be formed by pressing or sintering depending on the physical properties of the starting powder material. As a solid pellet was preferred to powder materials inside our electrochemical cell, the LMS-1 lunar simulant was sintered. Pellets of LMS-1 (24 g) were placed in a cylindrical alumina crucible and sintered using a furnace temperature of 1135 °C for 2 hours under an argon atmosphere. The samples resulting from this process were porous solid pellets approximately 46 mm in diameter and 10 mm tall, as shown in Figure 2.

Figure 2: Sintered pellet of LMS-1 lunar regolith simulant, 46 mm diameter and 10 mm thick.

Salts and oxides

Multiple electrolyte compositions were tested at different temperatures; Table 3 summarises these combinations. $CaCl_2$ was first chosen as a baseline electrolyte for its low cost and low toxicity, the

extensive number of studies that have been published with this electrolyte, and its availability. For $CaCl_2$-X (X=KCl, NaCl, LiCl) experiments, one experiment was performed at the reference working temperature of $CaCl_2$ (950 °C) and one with the same difference in temperature relative to its melting point as the difference between 950 °C and the melting point of $CaCl_2$, i.e., melting point + 180 °C. The mass of CaO and regolith to salt ratio was kept constant. The 1:33 ratio corresponds to the reduction of a 24 g lunar regolith simulant sintered pellet in 800 g of salt.

An experiment in LiCl with 0.8% Li_2O was performed at its melting point + 180 °C, for comparison purposes with the $CaCl_2$-based experiments. Although the electrolyte and oxide are different, LiCl is often presented as an alternative to $CaCl_2$ for reducing oxides at temperatures as low as 650 °C [19], [20].

Before each experiment, the salt was dried under vacuum at 120 °C for 48 h; this step lowers the amount of oxide formation (e.g., CaO) resulting from the hydrolysis of absorbed moisture.

Table 3: Salt, oxides and temperature combinations. All experiments have a regolith to salt ratio of 1:33 and used a mass of regolith of 24 g.

Salt	**Temp. (°C)**	**Oxide**
$CaCl_2$	950	0.8 wt% CaO
$CaCl_2$	900	0.8 wt% CaO
$CaCl_2$	850	0.8 wt% CaO
$CaCl_2$ (82 wt.%) /KCl (18 wt.%)	950	0.8 wt% CaO
$CaCl_2$ (82 wt.%) /KCl (18 wt.%)	806	0.8 wt% CaO
$CaCl_2$ (69 wt.%) /NaCl (31 wt.%)	950	0.8 wt% CaO
$CaCl_2$ (69 wt.%) /NaCl (31 wt.%)	680	0.8 wt% CaO
$CaCl_2$ (60 wt.%) /LiCl (40 wt.%)	950	0.8 wt% CaO
$CaCl_2$ (60 wt.%) /LiCl (40 wt.%)	660	0.8 wt% CaO
LiCl	785	0.8 wt% Li_2O

Electrochemical setup

The experimental setup consisted of a vertical 2.3 L Inconel 600 cell, with a removable lid at the top end. A 0.5 L alumina crucible filled with the dry salt and oxide was placed at the bottom of the cell. The cell was then sealed at the top with the lid, which has one inlet and one outlet for gas flow, two feedthroughs for the cathode basket, a further feedthrough for the anode, and a final feedthrough for a thermocouple. A two-electrode set-up was used for all experiments. The cathode was a Ø47 mm SS316 basket containing the sintered LMS-1 pellet, which was perforated with Ø2 mm holes to allow a sufficient flow of electrolyte during the process. The anode was a Ø12.7 mm graphite rod, 100 mm long. Both anode and cathode were connected to Inconel 600 rod current collectors. A K-type Inconel 600 thermocouple was covered with an alumina sheath and immersed in the salt. A water heat exchanger cooled the top of the cell, while the bottom was placed inside a tube furnace and the temperature was controlled to achieve the desired process temperature, between 660 °C and 950 °C. Figure 3 shows a sketch of the setup.

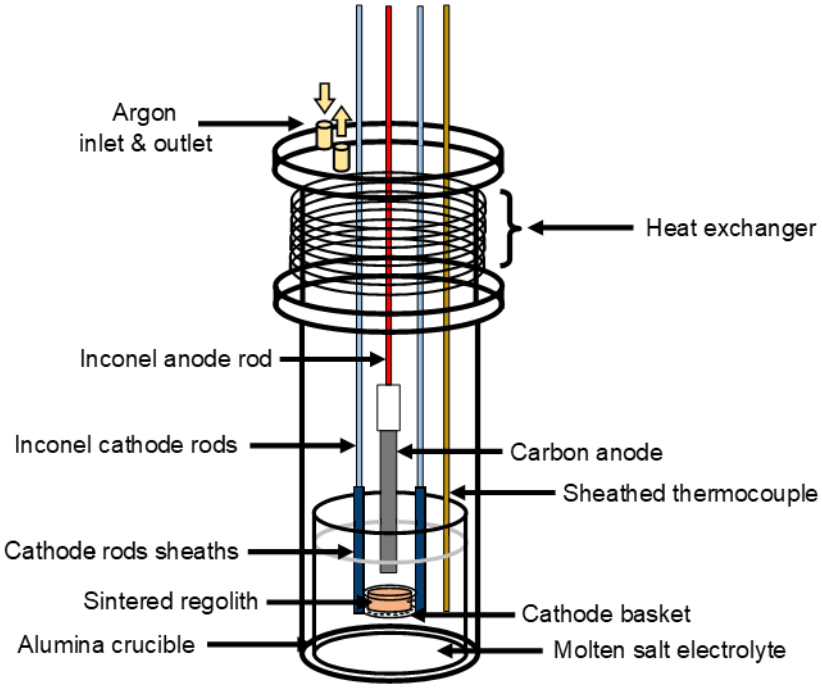

Figure 3: Sketch of the electrochemical cell

Reduction experiments

All reduction experiments were carried out using 24 g of LMS-1 and a constant voltage of 3.2 V for 24 hours; the voltage was ramped at a rate of 0.25 V/min at the start of each experiment. The electrolyte composition and temperature were varied as outlined in the previous sections. Electrolysis was controlled and monitored using a Biologic VMP3 with a 20 A booster; temperature was monitored using a Pico Technology data logger. A constant flow of argon (1 L/min) was used to maintain an inert atmosphere and facilitate the removal of process gasses from the reactor, which were filtered and qualitatively analysed by using a Pfeiffer Thermostar mass spectrometer.

Sample analysis

The recovered reduced samples were first washed with running water to remove most of the salt. Highly reduced samples were in a powder form as shown in Figure 4, while poorly reduced ones were still in the form of the original sintered pellet. The latter were therefore crushed into a powder for further washing with running water. Each sample was then washed with distilled water and filtrated before being vacuum dried at 120 °C for 24 h. A representative portion of each sample was embedded in epoxy resin, polished, and sputter coated with Pt-Au for analysis using a Scanning Electron Microscope (SEM) - Carl Zeiss EVO combined with an Oxford instruments X-Max Energy Dispersive X-ray (EDX). EDX was used to identify metallic phases of the reduced materials. A few mg of each sample was analysed by inert gas fusion using an Elementar® Inductar OHN Cube to measure the quantity of oxygen remaining in the reduced sample.

Figure 4: LMS-1 lunar simulant reduced in $CaCl_2$ at 950 °C

Results & discussions

Theoretical assessment

In the FFC Cambridge process, the applied voltage must be sufficient to reduce the oxides in the feedstock material, but below the deposition voltage of the alkali metal (Li, Na, K) or alkaline earth metal (Ca) chlorides that compose the electrolyte [32]. The decomposition voltage, of a given oxide or chloride is calculated based on the Gibbs free energy of the decomposition. Figure 5 shows the decomposition voltage for each electrolyte used in this work and for the main oxides that comprise lunar regolith. Simple oxides rather than actual minerals were used due to the availability of the thermodynamic data. They have been shown to be a relevant proxy in this application as the complex minerals likely decompose to simple oxides in the early stage of the reduction process [11], [33]. Given the temperature and electrolyte composition of the different experiments, the chosen voltage (3.2 V) should theoretically allow for oxygen extraction from all targeted oxides, yet not foster the decomposition of the electrolyte.

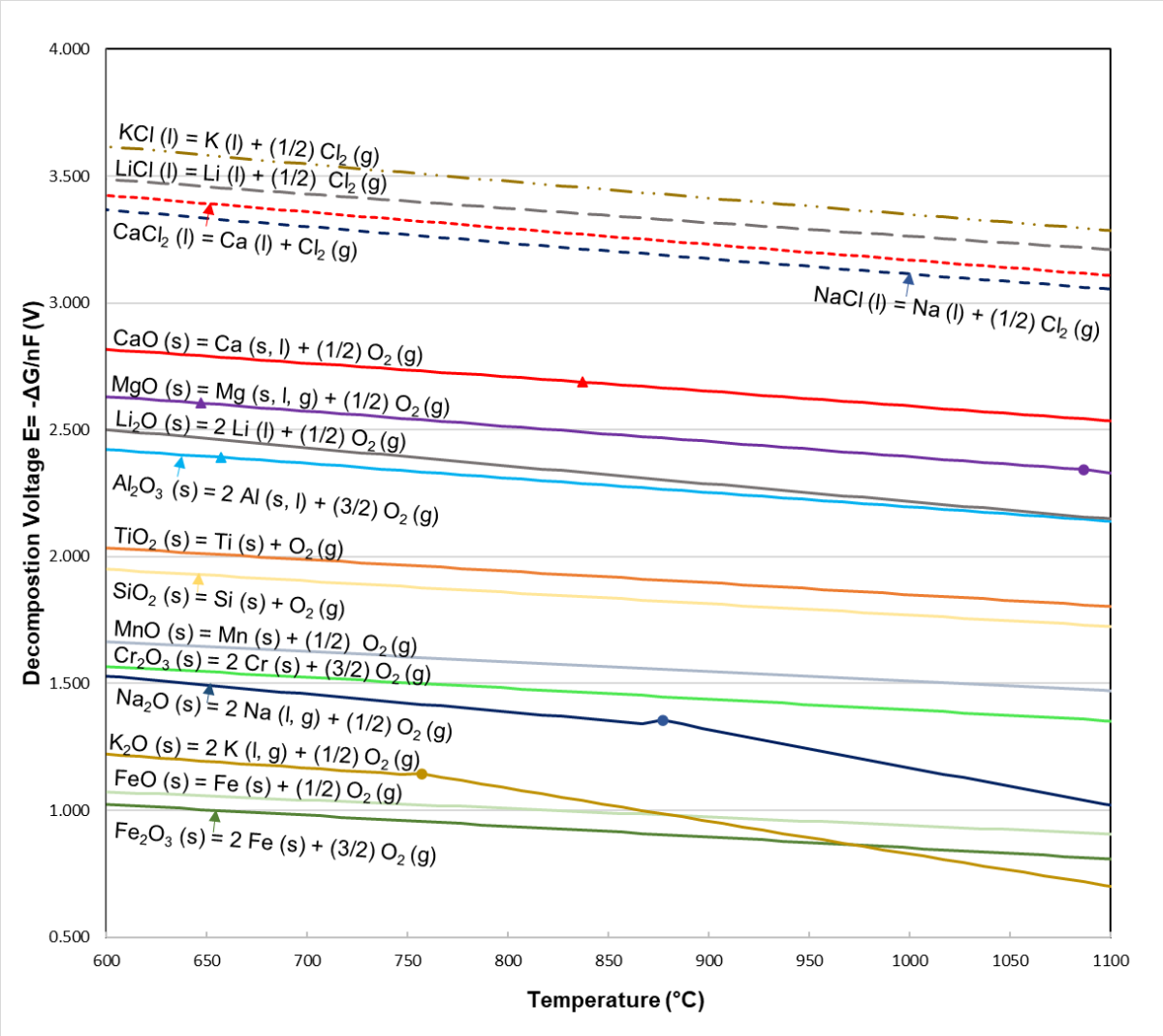

Figure 5: Decomposition voltage of oxides composing the regolith (solid lines) and the salts used as electrolytes in this work (dash lines) versus temperature. Transitions to liquid and to gas are indicated by a triangle and a circle, respectively.

Temperature-dependent oxygen extraction efficiency

Data summarising the oxygen content in reduced samples and the corresponding current efficiencies are plotted in Figure 6. Current efficiency, or Faradic efficiency, represents the fraction of electrons participating to the reduction. The first observation that can be made is that, while a high level of reduction of LMS-1 can be achieved in $CaCl_2$ at 950 °C (~85 %), reducing the temperature, in pure $CaCl_2$ and through the utilisation of eutectic mixtures, significantly impacts the achievable level of reduction in an equivalent processing time. However, more than 40% reduction of the lunar regolith simulant was achieved at 660 and 680 °C in the $CaCl_2$-LiCl and $CaCl_2$-NaCl eutectics, respectively, which is highly promising as this represents a significant reduction level at relatively low temperatures. The current efficiency also varies considerably between approximately 35 and 60%, depending on the temperature and salt composition. The extent of reduction in LiCl does not exceed

20%, with a current efficiency below 10%, thus highlighting the importance of electrolyte selection when targeting regolith reduction.

Comparison of current efficiencies between the different electrolyte compositions is challenging as the efficiency would be expected to change over the course of the reduction. At the start of the reduction, many of the oxides in regolith will form Ca-based intermediates; as current is used to drive the incorporation of Ca into the feedstock rather than extract any oxygen, the current efficiency may be lower in this initial stage. Similarly, towards the end of the reduction the current efficiency is also expected to be lower as the final % of oxygen is typically the hardest to remove from solid oxides [34]. As such, the current efficiency is likely to be highest part-way through the reduction process. As a different level of reduction was achieved in each electrolyte, direct comparison therefore does not necessarily reflect the entire story regarding influence of electrolyte composition. Nevertheless, some tentative conclusions can be drawn from the data presented in Figure 5. The current efficiency of reduction in pure $CaCl_2$ decreases with temperature; as the efficiency would be expected to be lower for the more complete reduction achieved at 950 °C, it is fair to say that current efficiency is negatively impacted if the temperature of that electrolyte is reduced. This point will be examined in greater detail in the following section. Comparing the reduction in $CaCl_2$ at 850 °C with $CaCl_2$-NaCl and $CaCl_2$-KCl (which all achieve a reduction level within approximately 10% of each other), it appears that the low temperature current efficiency can be improved through the use of eutectic salt mixtures. Regardless, the current efficiency of a shorter experiment reaching ~50% reduction in pure $CaCl_2$ at 950 °C may still be higher than the eutectic mixtures.

The lower percentage of extraction at lower temperatures was to be expected, given that higher temperatures reduce the kinetic barriers of the reduction, reduce the theoretical decomposition voltage of all oxides, and increase the solubility of ions in the molten salt [32]. These mechanisms, and others that impact the efficiency at different temperatures, will be discussed for each electrolyte composition in the subsequent sections. A closer analysis of the partially reduced material in each electrolyte will be presented, to assist in explaining the differences observed. The lower reduction percentages shown in Figure 6 represent a slower reduction rate, comparative to the reduction in $CaCl_2$ at 950 °C; whether these yields also reflect an upper limitation to the reduction possible at those temperatures is yet to be seen. It is anticipated that longer reduction times would enable higher yields at low temperatures.

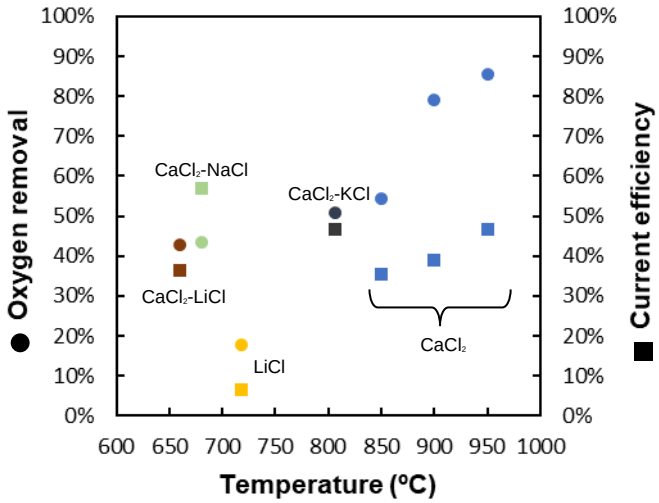

Figure 6: Oxygen removal by the molten salt electrolysis process in different salts and the associated current efficiency. Each colour represents a different salt composition (blue = $CaCl_2$; black = $CaCl_2$-KCl; green = $CaCl_2$-NaCl; brown = $CaCl_2$-LiCl; yellow = LiCl).

$CaCl_2$ electrolyte

$CaCl_2$ experiments have been extensively studied in the literature [11], [12], [35], [36]. The electro-deoxidation of the oxides follows reaction (1).

$M_xO_y + 2y\ e^- = xM + yO^{2-}$ (1)

The reduction process can be enhanced by calciothermic reduction as described in the Ono-Suzuki (OS) process [37]. Reactions (2), (3) and (4) describe the OS process. Calcium metal is generated at the cathode from the decomposition of CaO, rather than the $CaCl_2$ electrolyte, as shown by reactions (2) and (3) and can calciothermically reduce metal oxides by reaction (4). The newly formed CaO is then recycled by reaction (2), decomposing electrochemically between 2.5 and 2.7 V as shown in Figure 5.

$CaO = Ca^{2+} + O^{2-}$ (2)

$Ca^{2+} + 2e^- = Ca$ (3)

$M_xO_y + yCa = xM + yCaO$ (4)

In practice, many oxides will form intermediates during the electrochemical reduction, for example TiO_2:

$TiO_2 \rightarrow Ti_3O_5 \rightarrow Ti_2O_3 \rightarrow TiO \rightarrow Ti - O$ [38]–[40]

Calcium can also enter into the composition of some oxides to form intermediates [40], creating CaM_xO_y phases that can be less stable and easier to reduce (e.g., $CaTiO_x$ [39], [40]). On the other hand, some intermediates can be more thermodynamically stable and can require a higher potential to free the oxygen, as found in lithiothermic reductions which follow the same mechanisms (e.g.,

$LiAlO_2$ [36]). The formation of Ca and Li intermediates happens both chemically and electrochemically [39].

Following the electro-deoxidation of oxides and intermediates at the cathode, the extracted oxygen anions dissolve in the salt electrolyte. The dissolved oxygen anions migrate to the anode and are discharged as O_2, reaction (5), when an inert or oxygen-evolving anode is used (e.g., SnO_2), or as CO and CO_2, reactions (6) and (7), when a graphite anode is used, such as in the present study.

$2\ O^{2-} = O_2 + 4\ e^-$ (5)
$C + 2O^{2-} = CO_2 + 4e^-$ (6)
$C + O^{2-} = CO + 2e^-$ (7)

After 24h of electrolysis, the reduced LMS-1 simulant was observed by SEM, and phases were identified by EDX. Figure 7 shows one of the reduced grains. Ca/Si/Al and Fe/Ti/Si/Al phases can be identified. These phases were already observed in a reduced JSC-2A sample [11], and could originate from a plagioclase mineral coexisting in a grain with glass or titanomagnetite. A wide Si/Mg phase is, however, new to the authors, as similar phases previously identified also contained Ca and/or Al. This could indicate that the grain was richer in forsterite (olivine) or enstatite (pyroxene) or could represent a different stage in the reduction mechanism where Ca has not yet been incorporated or has already been expelled from the phase. While the similarity between reduced phases in LMS-1 and JSC-2A is fascinating, particularly as they have quite different original compositions, more experiments (including partial reductions) will be required in the future to understand the detailed reduction path of LMS-1 minerals. However, that analysis was not within the scope of the current study.

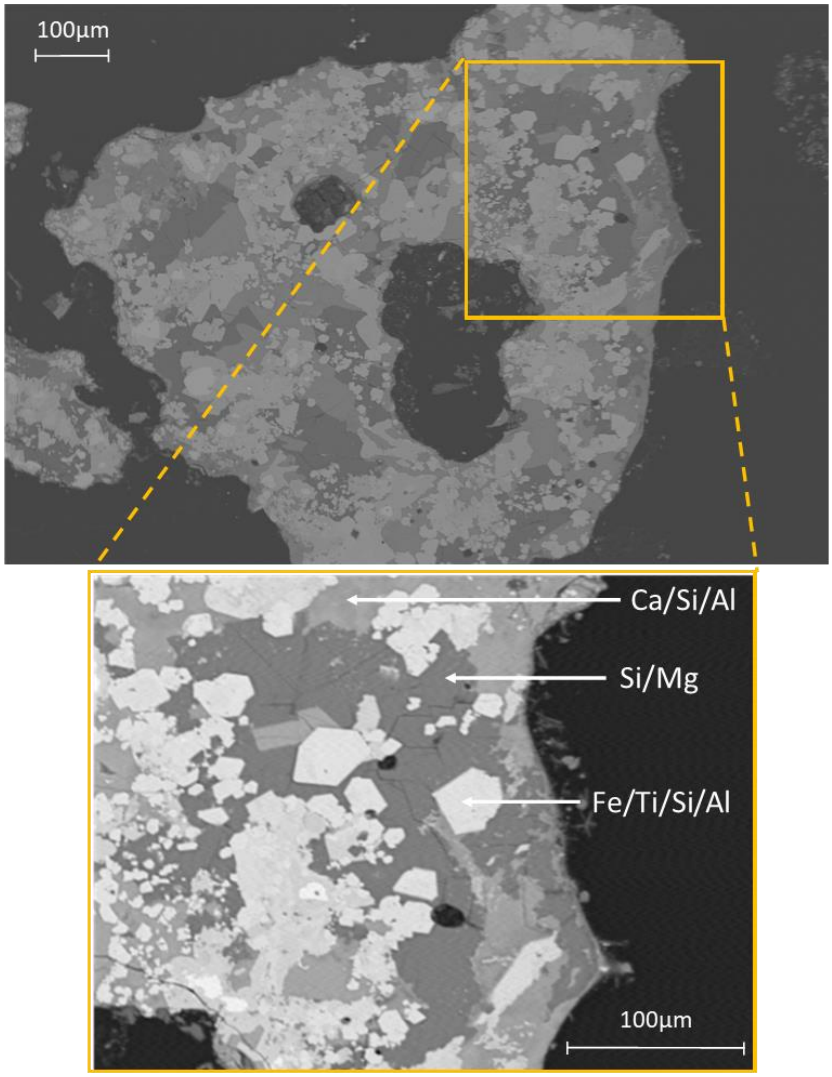

Figure 7: Back-scattered SEM image of an LMS-1 particle electrochemically reduced in $CaCl_2$ at 950 °C. Metal phases were identified by EDX.

Overall, the results of the baseline experiment with $CaCl_2$ at 950 °C as electrolyte are in line with what has already been published by Lomax et al. [11], with the majority (85 %) of the lunar regolith simulant being reduced to a metal powder in 24 hours. Any difference to the previously reported work can be explained by the use of a different lunar simulant, a different concentration of CaO in the electrolyte, a different salt to regolith ratio, and a different anode. Optimising the $CaCl_2$ experiment was, however, not the focus of this work. A longer reduction time would naturally have achieved an even more complete reduction, however, 24h was a convenient duration to use when comparison between different parameters was the primary goal.

Experiments at 850 °C and 900 °C in $CaCl_2$ show the impact of temperature on the reduction and current efficiency, in the absence of any effects from using a different electrolyte composition. Approaching the lower temperature limit imposed by the melting point of $CaCl_2$, the extent of reduction dropped to 50% and the current efficiency to less than 40%, from approximately 85% and 48%, respectively. When reducing insulating and semi-conducting oxides, higher temperatures help to lower the kinetic barriers to the reduction of the solid [32]. Additionally, as all experiments were carried out potentiostatically, the average current and resulting total charge can have a significant

impact on the reduction rate. For example, the total charge passed at 900 °C was ~8% less than at 950 °C, under equivalent conditions, while the total charge was reduced by ~40% at 850 °C. Clearly, a lower average current is going to result in a slower reduction rate. Furthermore, as species in the molten electrolyte will be less effected by the kinetic barriers imposed on the solid materials at low temperatures, relatively more parasitic cycling reactions may occur, which is reflected in the reduced current efficiency.

Two major parasitic cycling reactions exist in the FFC process. The first is linked to the formation of carbonates following reactions (8), (9), and (10). Dissolved CO_2 can react with O^{2-} (or CaO) to form carbonate anions (or calcium carbonate), which remains dissolved in the electrolyte and can subsequently reduce at the cathode to free O^{2-}. These ions can then be re-oxidised at the anode, thus creating a redox cycle where the current is not utilised for oxide reduction. The deposition of carbon at the cathode can contaminate the product and can also result in an accumulation at the surface of the melt. The accumulation of conductive carbon particles can create new paths for the current between the anode and cathode, further reducing the overall current efficiency.

At the anode:

$2O^{2-} + C = CO_2 + 4e^-$ (8)

$CO_2 + O^{2-} = CO_3^{2-}$ (9)

At the cathode

$CO_3^{2-} + 4e^- = C + 3O^{2-}$ (10)

Chen et al. [39] report that $CaCO_3$ decomposes to CO_2 and CaO at 887 °C, hence the accumulation of CO_3^{2-} in the melt and the parasitic cycling is limited at higher temperatures. Such a parasitic reaction would, however, not exist with inert anodes (which contain no carbon), hence the need to also advance the research on this part of the process.

The second cyclic reaction is linked to the dissolved calcium in the melt and is expressed by reactions (11) and (12). Ca^{2+} in the melt is reduced at the cathode to Ca metal, which dissolves into the melt. Ca^{2+} can subsequently reform at the anode. As with the previous example this process consumes current but does not contribute to the reduction of the regolith at the cathode. Additionally, Ca metal dissolved in the salt increases the electrical conductivity of the melt, thus lowering the current efficiency [41].

At the cathode:

$Ca^{2+} + 2e^- = Ca$ (11)

At the anode

$Ca = Ca^{2+} + 2e^-$ (12)

Cyclic reactions and kinetic barriers can explain the lower level of reduction of the lunar simulants after 24 h of electrolysis at temperatures below 950 °C. However, as previously discussed, the results in Figure 5 likely do not represent the limit of the reduction process under these conditions, and higher recovery percentages (mass of oxygen extracted per mass available) are to be expected with experiment durations longer than 24 h.

$CaCl_2$ – KCl eutectic electrolyte

The $CaCl_2$-KCl electrolyte was tested using an 82-18 wt.% mixture, with the first eutectic point at 626 °C according to the $CaCl_2$-KCl binary phase diagram. Besides lowering the electrolyte temperature, the KCl has the advantage that it is dissociated at higher voltage (3.44 V) compared to $CaCl_2$ (3.25 V). CeO_2, K_2CrO_4 and Ta_2O_5 reduction experiments have been previously performed with $CaCl_2$-KCl

mixtures [42]–[45]. Several limitations of oxides' reduction in this electrolyte compared to in pure $CaCl_2$ were identified in those studies, which may also apply in the present work.

Firstly, although the current efficiency of the $CaCl_2$-KCl experiments, around 45%, is similar to that of $CaCl_2$ at 950 °C, a lower efficiency is to be expected if the process was run for a longer time to achieve a reduction closer to 100%. The efficiency is, however, better than the reduction of LMS-1 in $CaCl_2$ at 850 °C, which achieved a similar reduction level. The anticipated lower efficiency compared to equivalent reduction levels in $CaCl_2$ at 950 °C likely emanates from similar causes as that seen in low temperate pure $CaCl_2$ electrolyte: the current efficiency of the $CaCl_2$-KCl eutectic is potentially limited further due to the higher solubility of CO_2 and CO_3^{2-} than in $CaCl_2$, and cycling reactions linked to the dissolved calcium in the melt. According to Claux [42], who performed experiments with both graphite and platinum (inert) electrodes, the calcium cycling reaction is primarily responsible for the loss in current efficiency in $CaCl_2$-KCl eutectic. Reduction mechanisms are otherwise expected to be like the reduction in $CaCl_2$, with direct electro-deoxidation and formation of intermediates with Ca.

SEM analyses of the samples reduced in $CaCl_2$-KCl at 806 °C are shown in Figure 8. Unlike the lunar simulant reduced in $CaCl_2$, it was not possible to find any metallic phases. The reduction (~51%) seemed to have been homogeneously distributed and progressed to only form intermediates, rather than reducing specific minerals more than others. Some calcium-rich phases could indicate calcium deposition and/or intermediate formation during the reduction of the minerals. The lack of small metallic iron areas that are typically seen in partially reduced LMS-1 in $CaCl_2$ is interesting, as these would be expected with a 50% level of reduction. In the literature, the identification of intermediates in the reduction of complex minerals was investigated by Zou et al. [33], who reduced pyroxenes and perovskite. At the beginning of the reduction, the following intermediates could be identified: $Ca_{12}Al_{14}O_{33}$, $CaTiO_3$, $MgAl_2O_4$, $CaSiO_3$. Such intermediates would then reduce and form sub-oxides with less oxygen in a process similar to the TiO_2 intermediates presented above. While the identification and quantification of intermediate phases was out of the scope of the present work, it is likely that similar intermediate species would form throughout the reduction of LMS-1 in all different eutectic mixtures. It is possible that different reduction intermediates or iron containing sub-oxides form in the electrolyte containing potassium, or that the iron components are lost into the salt somehow; these mechanisms could be assessed in more depth in future work if this eutectic mixture was used.

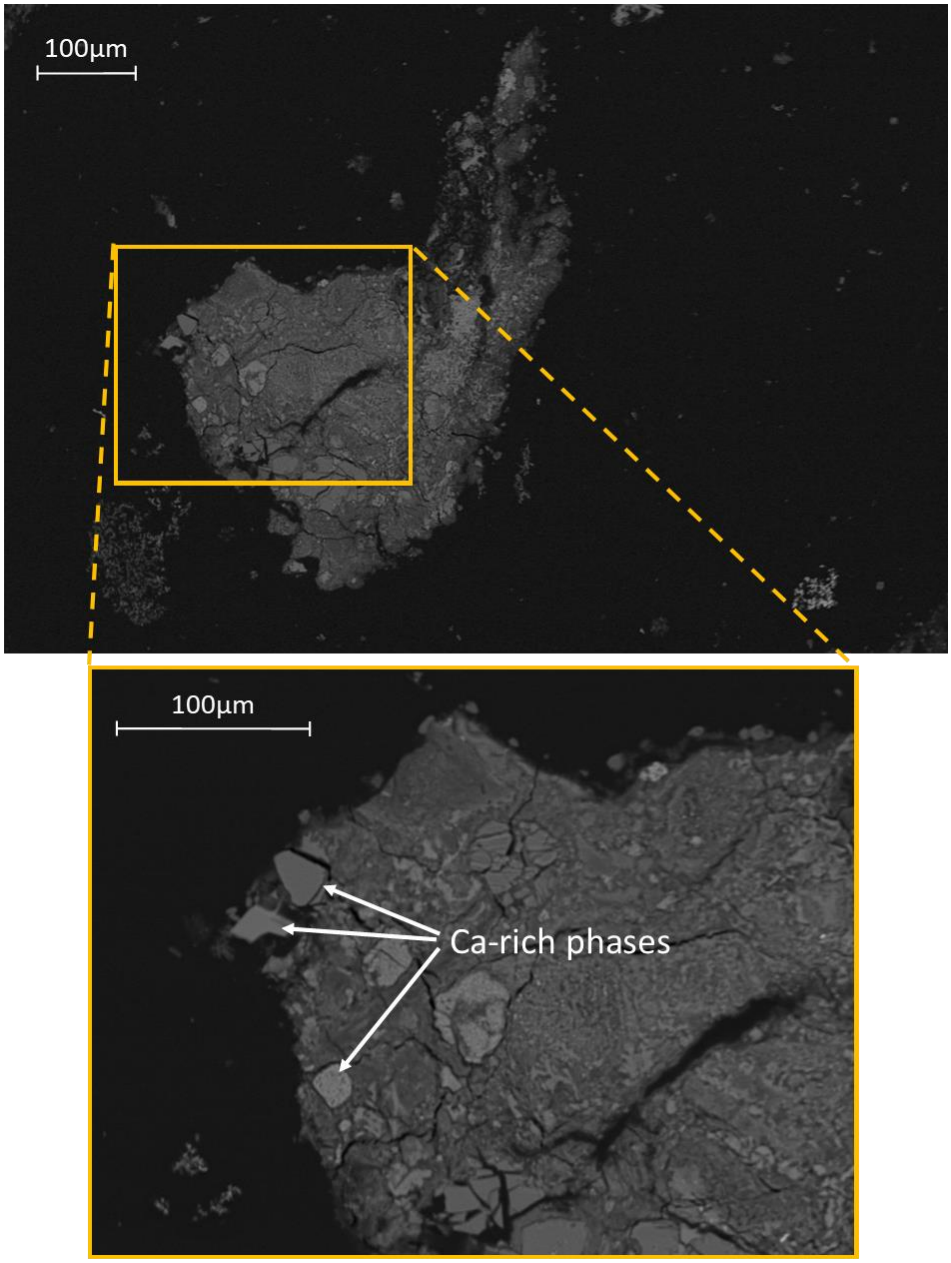

Figure 8: Back-scattered SEM image of an LMS-1 particle electrochemically reduced in $CaCl_2$-KCl eutectic at 806 °C. No pure metal phases could be identified.

$CaCl_2$ – NaCl eutectic electrolyte

$CaCl_2$-NaCl eutectics have been used to reduce many oxides, for example, ilmenite [23], Al_2O_3 [36], Cr_2O_3 [46], Ta_2O5 [47], GeO_2 [48], Nb_2O_5 [22] and UO_2 [49], the main advantage being the lower melting point of the electrolyte, which can be as low as 504 °C. All oxides in the regolith have a theoretical decomposition voltage lower than that of the salts composing this eutectic. In comparison to $CaCl_2$, $CaCl_2$-NaCl eutectic has a lower viscosity and a higher electrical conductivity, thus enhancing the diffusion and transport mechanisms within the electrolyte [22], [46]. The addition of NaCl to $CaCl_2$ should also reduce the CaO solubility and potentially prevent the regolith-based minerals and oxides from dissolving chemically into the electrolyte [22].

Although it would thermodynamically be possible, no NaM_xO_y intermediate was observed in the partially reduced LMS-1 product, which is in line with previous observations in the literature with more simple oxides [22], [46]–[48]. The low solubility of Na_2O in the eutectic compared to CaO, and the quick formation and growth of CaM_xO_y intermediates are hypothesised by Yan et al. [22] and Liu et al. [46] to be reasons for the lack of sodium-based intermediates. The sodium would, therefore, only be playing a passive role in the reduction. Experiments in pure NaCl have shown that essentially no reaction happens in this salt [23], [46], further reinforcing this hypothesis.

In this work, more than 40% of the regolith could be reduced at 680 °C, with a current efficiency above 60%. This offers a more efficient use of the current at a temperature 126 °C less than the $CaCl_2$-KCl eutectic, without a significant loss in reduction performance. No additional parasitic reactions could be identified from the literature study, thus explaining the good current efficiency compared to other melts.

The SEM observations are shown in Figure 9. At 680 °C, no metal-rich phase could be observed in any particle. Like the $CaCl_2$-KCl eutectic at 806 °C, all the phases are likely in an intermediate stage rather than particular components being fully metallised, thus leaving the reduced materials with structural changes not prominent enough to be observed by SEM and EDX. While metallic phases are quite distinct compared to oxides, EDX is not a quantitative method for oxygen analysis, which is why the reduction percentages are determined by the inert gas fusion method.

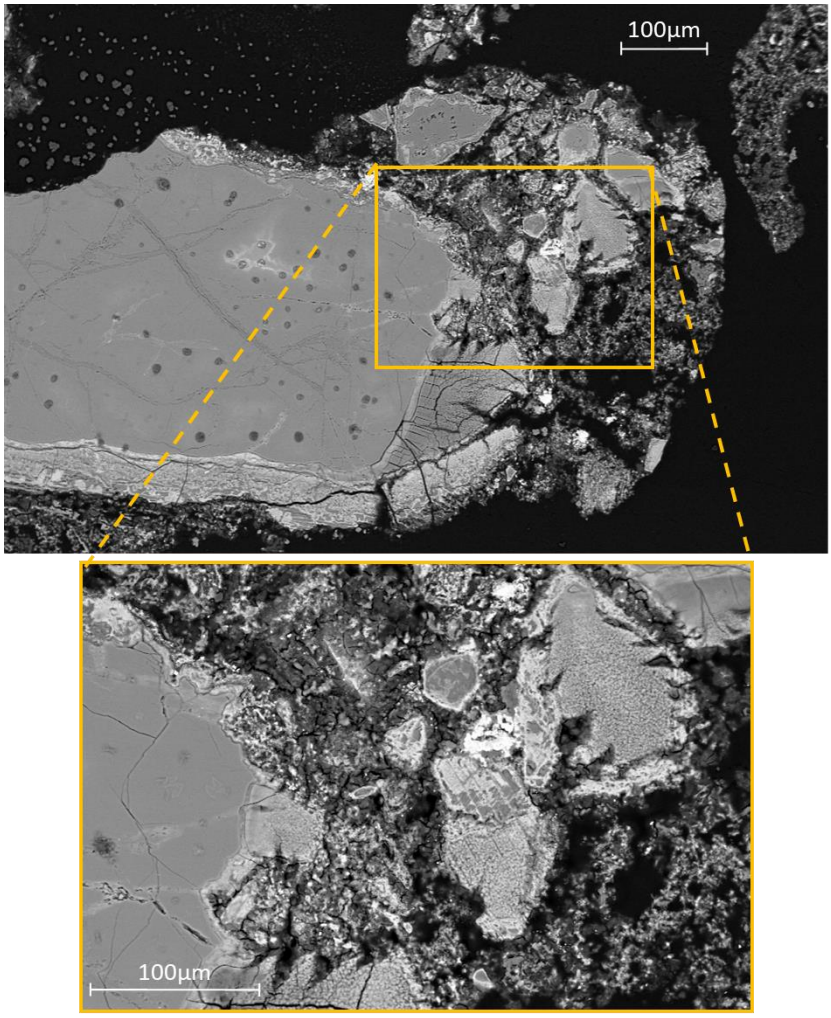

Figure 9: Back-scattered SEM image of an LMS-1 particle electrochemically reduced in $CaCl_2$-NaCl eutectic at 680 °C. No fully metallic phases were identified.

$CaCl_2$ – LiCl eutectic electrolyte

To the authors' knowledge, $CaCl_2$-LiCl eutectics have only been used to reduce Al_2O_3 [36], although LiCl has been used as a component of other eutectic salt mixtures. Like the addition of NaCl, the addition of LiCl to $CaCl_2$ allows a lower melting point and a higher electrical conductivity. Metallothermic reduction from dissolved Li and Ca (originating from the salt only or also the additional oxide, respectively) should also play a role in the overall reduction of the oxide.

The level of reduction at 660 °C in $CaCl_2$-LiCl eutectic, above 40%, was similar to the $CaCl_2$-NaCl eutectic but the current efficiency dropped to approximately 35%. Since no parasitic reaction specific to the $CaCl_2$-LiCl eutectic could be identified, the low current efficiency is expected to come from similar parasitic reactions to the ones occurring in LiCl, which are explained below.

SEM and EDX analysis in Figure 10 show evidence of metallised metal phases, such as Si/Ca and Si/Ti/Fe. It is, however, difficult to know which minerals and reductions paths led to these phases and why they are more evident than in the previous eutectic examples with similar reduction levels. A partially reduced olivine mineral could also be identified; as the grain contained all the elements

present in olivine, but a much lower fraction of oxygen compared to non-reduced LMS-1 olivine analysed by the same method, it is reasonable to assume that this phase is partially reduced.

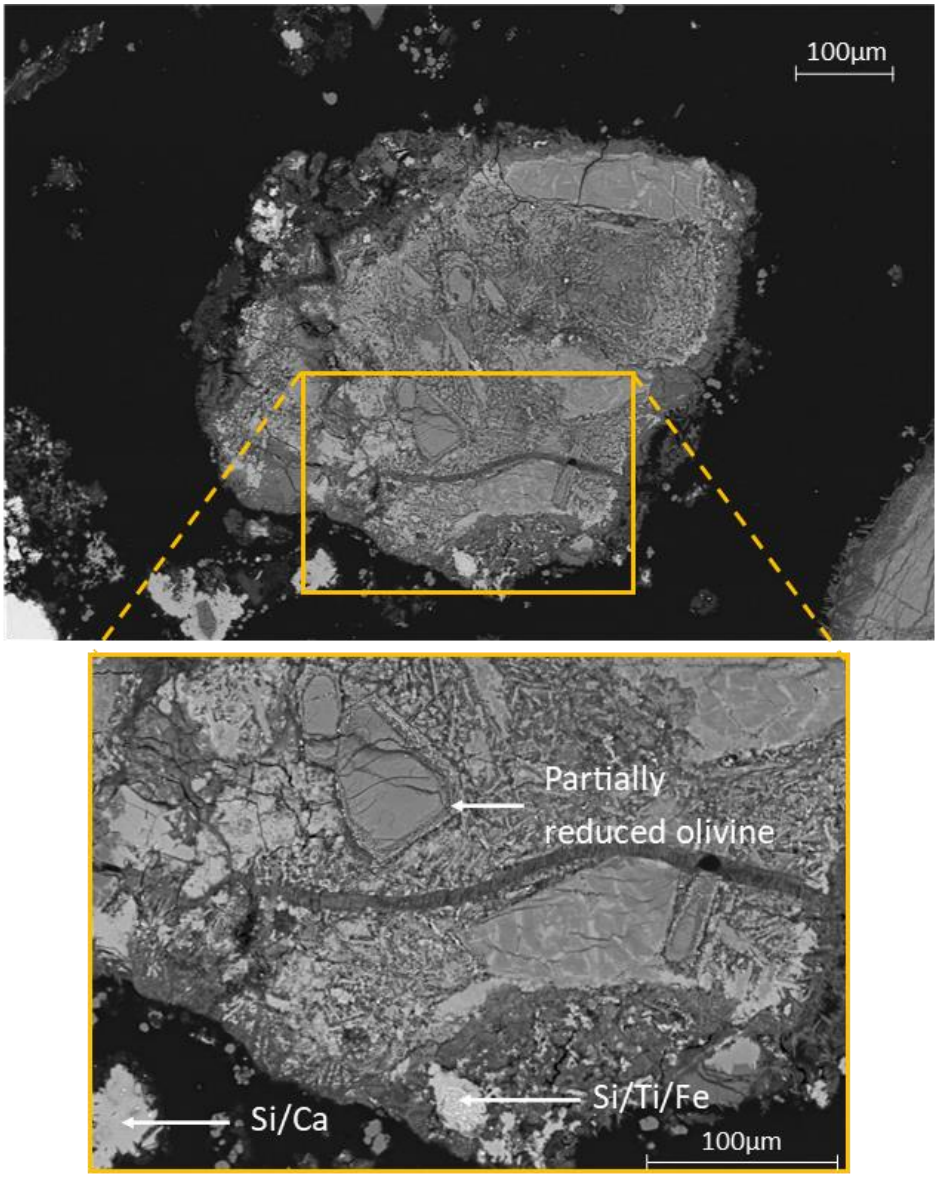

Figure 10: Back-scattered SEM image of an LMS-1 particle electrochemically reduced in $CaCl_2$-LiCl eutectic at 660 °C. Metallic phases were identified by EDX.

LiCl electrolyte

LiCl is often considered as an alternative electrolyte to pure $CaCl_2$ and $CaCl_2$-based eutectic mixtures [14], [19], [50]–[55]. Similar reduction mechanisms to $CaCl_2$ are to be expected, with combined electrodeoxidation and metallothermic reduction as well as the formation of Li-based intermediates, yet the temperature can be lower as the melting point of LiCl is 605 °C, which is the main incentive to perform experiments in pure LiCl. Reaction (1) drives the electrodeoxidation just like in $CaCl_2$-based experiments, and Li_2O can decompose following reactions (13) and (14) to allow

metallothermic reduction with Li metal deposited on the regolith cathode, as expressed by reaction (15). Li_2O can however decompose more easily than CaO, the decomposition voltage of Li_2O being below 2.5 V, compared with about 2.8 V for CaO. Oxygen ions can migrate to the anode and oxidise as O_2 or CO_2 gas, like in $CaCl_2$-based electrolytes.

$Li_2O = 2Li^+ + O^{2-}$ (13)

$Li^+ + e^- = Li$ (14)

$M_xO_y + 2yLi = xM + yLi_2O$ (15)

During the reduction process, intermediates with intercalated Li are expected to form faster in LiCl than in other studied molten salts because of the smaller size of Li^+ ions compared to Ca^{2+}, allowing for the formation of intermediates deeper in the material's structure [56].

Although LiCl experiments do not necessarily have the same optimal parameters as $CaCl_2$-based ones, the experiment was carried out for comparison purposes in the same conditions: with a carbon anode, and at 180 °C above its melting point. 0.8 wt.% of Li_2O was added instead of CaO. Results show a reduction level below 20% and a current efficiency of 6%.

The relatively low level of reduction compared to the other experiments carried out in this work can be explained by a saturation of deposited Li metal at the cathode [53], and potentially the lower oxide solubility at the operating temperature, which is discussed further in the subsequent section. In addition, intermediates with high thermodynamic stability could also be a barrier to the oxide reduction. The formation of the stable compound $LiTiO_2$ during titanium oxide electroreduction in LiCl was hypothesised by Qiu et al. [56] to explain the poor extent of reduction. Some experimental observations support this hypothesis as increasing the voltage slightly above 3.4 V led to a new release of oxygen according to our gas analysis. This test could however not be carried out for more than a few minutes since, as expected from the salt decomposition voltage, chlorine gas was forming at this voltage.

The extremely low current efficiency is linked to the carbonate cycle which has a more detrimental impact on the process than in $CaCl_2$-based electrolytes. CO_3^{2-} is stable in LiCl at extremely low O^{2-} concentrations and CO_2 partial pressures [57]. The salt becomes quickly saturated with carbon particles from reaction (9) and the current by-passes the regolith completely.

No SEM was performed on the reduced sample as the level of reduction was considered too low to be noticeable. Regardless of the achieved reduction, an additional challenge with LiCl is that Li deposition or inclusion in metal oxides is not visible by EDX due to the low atomic mass of lithium.

If an appropriate inert anode is identified, new experiments in LiCl should be carried out with the voltage interrupted periodically to prevent an excessive deposition of Li. Too much Li deposition at the surface of the cathode product could block O^{2-} transport as well as Li_2O diffusion and dissolution. The interruption allows the Li metal already deposited at the cathode to dissolve as Li^+ in the electrolyte, thus preventing excessive amounts from stopping the electroreduction. This technique has shown promising results to reduce TiO_2 [53].

$CaCl_2$ content and CaO solubility

At this stage of the research with lunar regolith reduction in molten salt, it is still difficult to identify exactly which chemical and electrochemical reactions enhance or hinder the oxide reduction in different electrolyte mixtures. Potential parasitic reactions were identified but the lower reduction and current efficiency of the process below 950 °C could also be associated with another process parameter: the CaO solubility.

CaO increases the solubility of oxygen ions in the melt and contributes Ca^{2+} for intercalation in the cathode material [58], [59]. These features are expected to be critical to the reduction process. However, the solubility of CaO in the different eutectics changes significantly, for example decreasing from 16 wt.% in pure $CaCl_2$ down to 4 wt.% in equimolar $CaCl_2$-KCl mixtures at 950 °C [60]. Lower processing temperatures would lower the solubility even further. Insufficient solubility could lead to CaO locally exceeding the solubility limit and precipitating out the electrolyte during the process, potentially blocking pores of the cathode and significantly impacting the efficiency of the reduction or even halting it entirely. A low solubility of CaO could also lead to more Ca dissolved in the salts, as electrolyte decomposition may be necessary to maintain the flow of current; this would increase the calcium cycling parasitic reaction. Although the solubility of CaO in the eutectic melts of this work could not be measured directly, the eutectic experiments were all repeated at 950 °C to allow for a comparison under equivalent conditions, and the results are shown in Figure 11.

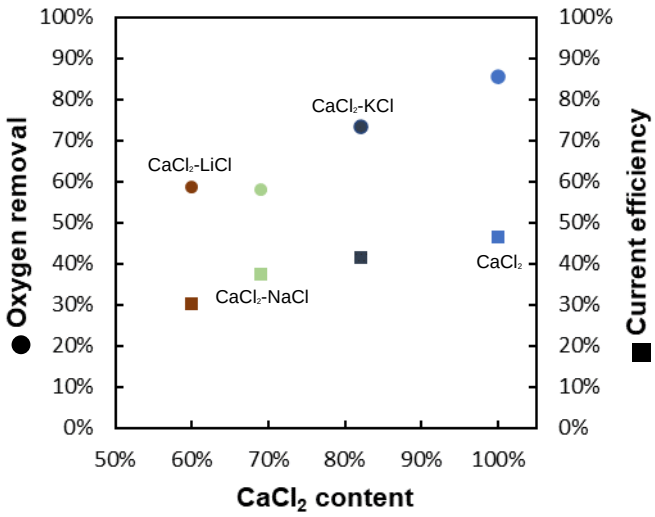

Figure 11: Oxygen removal by the molten salt electrolysis process and associated current efficiency at 950 °C versus $CaCl_2$ content. Each colour represents a different salt composition (blue = $CaCl_2$; black = $CaCl_2$-KCl; green = $CaCl_2$-NaCl; brown = $CaCl_2$-LiCl).

A trend can be noticed in Figure 10, whereby higher $CaCl_2$ content leads to more complete reduction and better current efficiency. The increase in CaO solubility may be responsible for this trend, highlighting the importance of CaO in the reduction process. Intermediates in pure $CaCl_2$ could also form and reduce more quickly, thus increasing the process efficiency. These results also clearly show that the lower level of reduction achieved with eutectics is not solely due to the lower process temperature reducing the kinetics of the reduction.

The high volatility of LiCl prevented an experiment at 950 °C form being run with this electrolyte. The Li_2O solubility in LiCl is 8.7 wt% at 650 °C [61], so the solubility of this oxide could also be a factor limiting the reduction in LiCl.

Conclusion

LMS-1 lunar regolith simulant was successfully reduced with various $CaCl_2$-based eutectic salts to at least 40% of the original oxygen content of the simulant. These reductions were carried out in 24 h, the baseline for a close to full reduction in pure $CaCl_2$. Reducing the temperature of $CaCl_2$ down to 850 °C dropped the current efficiency to below 30%. The use of eutectic mixtures at temperatures as low as 660 °C has shown the potential of reducing the process temperature below that which is possible in pure $CaCl_2$ while still maintaining a reasonable current efficiency and decent level of reduction in the given time. Longer experiments should be performed to assess the achievable maximum reduction, which could be limited kinetically or thermodynamically.

Carbonate formation in all studied electrolytes, and dissolved calcium in $CaCl_2$-based compositions are likely responsible for the observed parasitic reactions. The impact of these parasitic reactions is, however, linked to the respective solubility of these species in the electrolyte. $CaCl_2$-KCl is likely more significantly impacted by calcium cycling, while $CaCl_2$-LiCl and pure LiCl appear to be more sensitive to the dissolved carbonates. $CaCl_2$-NaCl seems in this regard the best alternative as no behaviour different from the pure $CaCl_2$ could be identified and a reasonable level of reduction was achieved at comparatively low temperatures, without significant loss of current efficiency.

Experiments with all eutectics at 950 °C have highlighted that the efficiency of the reaction is not only temperature driven, and that the $CaCl_2$ content and associated CaO solubility may be an important factor when targeting an efficient reduction.

Future work should focus on finding the reduction limit of these eutectics. Developing a new inert anode is also a priority, as it could allow more complete reductions in $CaCl_2$-LiCl and LiCl electrolytes and advance the process closer to space applications.

References

[1] ISECG, “Global Exploration Roadmap Supplement – Lunar Surface Exploration Scenario Update,” 2020.

[2] A. Meurisse and J. Carpenter, “Past, present and future rationale for space resource utilisation,” *Planet. Space Sci.*, vol. 182, no. January, p. 104853, 2020, doi: 10.1016/j.pss.2020.104853.

[3] D. S. Mckay and C. C. Allen, “Hydrogen reduction of lunar materials for oxygen extraction on the moon,” in *AIAA 34th Aerospace Sciences Meeting and Exhibit*, 1996, pp. 1–8, doi: 10.2514/6.1996-488.

[4] K. A. Lee, L. Oryshchyn, A. Paz, M. Reddington, and T. M. Simon, “The ROxygen Project: Outpost-Scale Lunar Oxygen Production System Development at Johnson Space Center,” *J. Aerosp. Eng.*, vol. 26, no. 1, pp. 67–73, 2013, doi: 10.1061/(ASCE)AS.1943-5525.0000230.

[5] D. L. Clark, B. W. Keller, and J. A. Kirkland, “Field test results of the PILOT hydrogen reduction reactor,” *Proc. AIAA Sp. Conf. Expo.*, no. September, p. AIAA 2009-6475, 2009.

[6] H. M. Sargeant *et al.*, “Hydrogen reduction of ilmenite: Towards an in situ resource utilization demonstration on the surface of the Moon,” *Planet. Space Sci.*, vol. 180, no. April 2019, p. 104751, 2020, doi: 10.1016/j.pss.2019.104751.

[7] C. C. Allen, R. V. Morris, and D. S. McKay, “Oxygen extraction from lunar soils and pyroclastic glass,” *J. Geophys. Res. E Planets*, vol. 101, no. E11, pp. 26085–26095, 1996, doi: 10.1029/96JE02726.

[8] E. E. Rice, S. D. Rosenberg, O. Musbah, P. A. Hermes, and P. A. Bemowski, “Carbothermal Reduction of lunar materials for oxygen production on the Moon: reduction of lunar simulants with carbon,” in *AIAA 34th Aerospace Sciences Meeting and Exhibit*, 1996, pp. 1–35, doi: 10.2514/6.1996-487.

[9] L. Schlüter and A. Cowley, “Review of techniques for In-Situ oxygen extraction on the moon,” *Planet. Space Sci.*, vol. 181, no. April 2019, p. 104753, 2020, doi: 10.1016/j.pss.2019.104753.

[10] L. A. Taylor and W. D. Carrier, “Oxygen production on the Moon: an overview and evaluation,” *Resources of Near-Earth Space*. pp. 69–108, 1993.

[11] B. A. Lomax, M. Conti, N. Khan, N. S. Bennett, A. Y. Ganin, and M. D. Symes, “Proving the viability of an electrochemical process for the simultaneous extraction of oxygen and production of metal alloys from lunar regolith,” *Planet. Space Sci.*, vol. 180, no. April 2019, p. 104748, 2020, doi: 10.1016/j.pss.2019.104748.

[12] C. Schwandt, J. A. Hamilton, D. J. Fray, and I. A. Crawford, “The production of oxygen and metal from lunar regolith,” *Planet. Space Sci.*, vol. 74, no. 1, pp. 49–56, 2012, doi: 10.1016/j.pss.2012.06.011.

[13] D. Fray and C. Schwandt, “Aspects of the Application of Electrochemistry to the Extraction of Titanium and Its Applications,” *Mater. Trans.*, vol. 58, no. 3, pp. 306–312, 2017, doi: 10.2320/matertrans.MK201619.

[14] Y. Sakamura, M. Kurata, and T. Inoue, “Electrochemical Reduction of UO2 in Molten CaCl2 or LiCl,” *J. Electrochem. Soc.*, vol. 153, no. 3, pp. 31–39, 2006, doi: 10.1149/1.2160430.

[15] D. Sri Maha Vishnu, N. Sanil, K. S. Mohandas, and K. Nagarajan, “Electrochemical characterisation of CaCl2 deficient LiCl-KCl-CaCl2 eutectic melt and electro-deoxidation of solid UO2,” *J. Nucl. Mater.*, vol. 470, pp. 179–186, 2016, doi: 10.1016/j.jnucmat.2015.12.003.

[16] Y. Sakamura, “Effect of alkali and alkaline-earth chloride addition on electrolytic reduction of UO2 in LiCl salt bath,” *J. Nucl. Mater.*, vol. 412, no. 1, pp. 177–183, 2011, doi: 10.1016/j.jnucmat.2011.02.055.

[17] K. S. Mohandas, “Direct electrochemical conversion of metal oxides to metal by molten salt electrolysis: a review,” *Miner. Process. Extr. Metall.*, vol. 122, no. 4, pp. 195–212, 2014, doi: 10.1179/0371955313z.00000000069.

[18] M. Iizuka, T. Inoue, M. Ougier, and J. P. Glatz, “Electrochemical reduction of (U, Pu)O2 in

molten LiCl and CaCl2 electrolytes," *J. Nucl. Sci. Technol.*, vol. 44, no. 5, pp. 801–813, 2007, doi: 10.1080/18811248.2007.9711869.

[19] S. C. Lee, J. M. Hur, and C. S. Seo, "Silicon powder production by electrochemical reduction of SiO2 in molten LiCl-Li2O," *J. Ind. Eng. Chem.*, vol. 14, no. 5, pp. 651–654, 2008, doi: 10.1016/j.jiec.2008.04.010.

[20] S. M. Jeong, H. Y. Yoo, J. M. Hur, and C. S. Seo, "Preparation of metallic niobium from niobium pentoxide by an indirect electrochemical reduction in a LiCl-Li2O molten salt," *J. Alloys Compd.*, vol. 452, no. 1, pp. 27–31, 2008, doi: 10.1016/j.jallcom.2007.02.057.

[21] S. M. Jeong, J. Y. Jung, C. S. Seo, and S. W. Park, "Characteristics of an electrochemical reduction of Ta2O5 for the preparation of metallic tantalum in a LiCl-Li2O molten salt," *J. Alloys Compd.*, vol. 440, no. 1–2, pp. 210–215, 2007, doi: 10.1016/j.jallcom.2006.05.139.

[22] X. Y. Yan and D. J. Fray, "Electrochemical Studies on Reduction of Solid Nb2O5in Molten CaCl2-NaCl Eutectic," *J. Electrochem. Soc.*, vol. 152, no. 10, p. E308, 2005, doi: 10.1149/1.2006567.

[23] Z. Zhou *et al.*, "Electrolytic synthesis of ferrotitanium powders from ilmenite in CaCl2-NaCl melts at a lower temperature of 700 °C," *J. Alloys Compd.*, vol. 726, pp. 1124–1131, 2017, doi: 10.1016/j.jallcom.2017.08.102.

[24] Y. shuai Wang *et al.*, "Electrolytic production of Ti-Ge intermetallics from oxides in molten CaCl2-NaCl," *Trans. Nonferrous Met. Soc. China (English Ed.*, vol. 28, no. 11, pp. 2351–2359, 2018, doi: 10.1016/S1003-6326(18)64880-0.

[25] L. Xiong *et al.*, "Effect of CaO addition on preparation of ferrotitanium from ilmenite by electrochemical reduction in CaCl2-NaCl molten salt," *J. Alloys Compd.*, vol. 676, pp. 383–389, 2016, doi: 10.1016/j.jallcom.2016.03.195.

[26] E. Ergül, S. Karakaya, and M. Erdoan, "Electrochemical decomposition of SiO2 pellets to form silicon in molten salts," *J. Alloys Compd.*, vol. 509, no. 3, pp. 899–903, 2011, doi: 10.1016/j.jallcom.2010.09.126.

[27] D. Vaniman, J. Dietrich, G. J. Taylor, and G. Heiken, "Exploration, Samples, and recent concepts of the Moon," in *Lunar sourcebook*, 1991, pp. 5–26.

[28] L. A. Taylor and T. T. Meek, "Microwave sintering of lunar soil: properties, theory, and practice," *J. Aerosp. Eng.*, vol. 18, no. 3, pp. 188–196, 2005.

[29] Exolith Lab, "LMS-1 Lunar Mare Simulant Fact Sheet," p. 2019, 2019, [Online]. Available: https://sciences.ucf.edu/class/simulant_lunarmare/.

[30] J. J. Papike, S. B. Simon, and J. C. Laul, "The lunar regolith: Chemistry, mineralogy, and petrology," *Rev. Geophys.*, vol. 20, no. 4, pp. 761–826, 1982, doi: 10.1029/RG020i004p00761.

[31] D. T. L. Alexander, C. Schwandt, and D. J. Fray, "The electro-deoxidation of dense titanium dioxide precursors in molten calcium chloride giving a new reaction pathway," *Electrochim. Acta*, vol. 56, no. 9, pp. 3286–3295, 2011, doi: 10.1016/j.electacta.2011.01.027.

[32] G. Chen, D. Fray, and T. Farthing, "Direct electrochemical reduction of titanium dioxide to

titanium in molten calcium chloride," *Nature*, vol. 407, no. 6802, pp. 361–364, 2000.

[33] X. Zou, X. Lu, Z. Zhou, C. Li, and W. Ding, "Direct selective extraction of titanium silicide Ti5Si3 from multi-component Ti-bearing compounds in molten salt by an electrochemical process," *Electrochim. Acta*, vol. 56, no. 24, pp. 8430–8437, 2011.

[34] G. Z. Chen and D. J. Fray, *Invention and fundamentals of the FFC Cambridge Process*. Elsevier Inc., 2019.

[35] C. Schwandt, D. T. L. Alexander, and D. J. Fray, "Electrochimica Acta The electro-deoxidation of porous titanium dioxide precursors in molten calcium chloride under cathodic potential control," vol. 54, pp. 3819–3829, 2009, doi: 10.1016/j.electacta.2009.02.006.

[36] X. Y. Yan and D. J. Fray, "Direct electrolytic reduction of solid alumina using molten calcium chloride-alkali chloride electrolytes," *J. Appl. Electrochem.*, vol. 39, no. 8, pp. 1349–1360, 2009, doi: 10.1007/s10800-009-9808-3.

[37] R. O. Suzuki, K. Teranuma, and K. Ono, "Calciothermic Reduction of Titanium Oxide and in-situ Electrolysis in Molten CaCl 2," *Metall. Mater. Trans. B*, vol. 34, no. 3, pp. 287–295, 2003.

[38] K. Dring, "Electrochemical Reduction of Titanium Dioxide in Molten Calcium Chloride," Imperial College of London, 2005.

[39] G. Z. Chen, "Interactions of molten salts with cathode products in the FFC Cambridge Process," *Int. J. Miner. Metall. Mater.*, vol. 27, no. 12, pp. 1572–1587, 2020, doi: 10.1007/s12613-020-2202-1.

[40] C.Schwandt and D.J.Fray, "Determination of the kinetic pathway in the electrochemical reduction of titanium dioxide in molten calcium chloride," *Electrochim. Acta*, vol. 51, no. 1, pp. 66–76, 2005.

[41] G. Z. Chen, "The FFC Cambridge process and its relevance to valorisation of ilmenite and titanium-rich slag," *Trans. Institutions Min. Metall. Sect. C Miner. Process. Extr. Metall.*, vol. 124, no. 2, pp. 96–105, 2015, doi: 10.1179/1743285514Y.0000000073.

[42] B. Claux, "Etude de la réduction électrochimique d ' oxydes d ' actinides en milieu sels fondus To cite this version : HAL Id : tel-00680359 Etude de la réduction électrochimique d ' oxydes d ' actinides en milieu de sels fondus," 2012.

[43] W. Weng, M. Wang, X. Gong, Z. Wang, D. Wang, and Z. Guo, "Direct electro-deposition of metallic chromium from K2CrO4 in the equimolar CaCl2-KCl molten salt and its reduction mechanism," *Electrochim. Acta*, vol. 212, no. 10, pp. 162–170, 2016.

[44] W. Weng, M. Wang, X. Gong, Z. Wang, D. Wang, and Z. Guo, "The Electrochemical Society, find out more Mechanism Analysis of Carbon Contamination and the Inhibition by an Anode Structure during Soluble K2CrO4 Electrolysis in CaCl2-KCl Molten Salt," *J. Electrochem. Soc.*, vol. 164, no. 12, 2017.

[45] A. A. Chernyshev, A. P. Apisarov, and P. Zaykov Yu., "Secondary reduction of tantalum in NaCl – KCl and KCl – CaCl2 molten salts," *Tsvetnye Met.*, 2017, doi: 10.17580/tsm.2017.11.08.

[46] Z. wei Liu *et al.*, "Direct electrolytic preparation of chromium metal in CaCl2–NaCl eutectic

salt," *Trans. Nonferrous Met. Soc. China (English Ed.*, vol. 28, no. 2, pp. 376–384, 2018, doi: 10.1016/S1003-6326(18)64671-0.

[47] Q. Song, Q. Xu, X. Kang, J. hong Du, and Z. ping Xi, "Mechanistic insight of electrochemical reduction of Ta2O5 to tantalum in a eutectic CaCl2-NaCl molten salt," *J. Alloys Compd.*, vol. 490, no. 1–2, pp. 241–246, 2010, doi: 10.1016/j.jallcom.2009.09.168.

[48] L. Rong, R. He, Z. Wang, J. Peng, X. Jin, and G. Z. Chen, "Investigation of electrochemical reduction of GeO2 to Ge in molten CaCl2-NaCl," *Electrochim. Acta*, vol. 147, pp. 352–359, 2014, doi: 10.1016/j.electacta.2014.09.107.

[49] D. Sri Maha Vishnu, N. Sanil, G. Panneerselvam, S. K. Mahato, K. V Soja, and K. S. Mohandas, "Factors Influencing the Direct Electrochemical Reduction of UO2 Pellets to Uranium Metal in CaCl2-48 mol % NaCl Melt Factors Influencing the Direct Electrochemical Reduction of UO 2 Pellets to Uranium Metal in CaCl 2 -48 mol % NaCl Melt," *J. Electrochem. Soc.*, vol. 160, no. August 2014, pp. 583–592, 2013, doi: 10.1149/2.024311jes.

[50] C. S. Seo, S. M. Jeong, S. Bin Park, J. Y. Jung, S. W. Park, and S. H. Kim, "Preparation of tantalum powder from Ta2O5 by an electrochemical reduction in an LiCl-Li2O molten salt system," *J. Chem. Eng. Japan*, vol. 39, no. 1, pp. 77–82, 2006, doi: 10.1252/jcej.39.77.

[51] E. Choi *et al.*, "Electrochemical reduction of UO 2 in LiCl – Li 2 O molten salt using porous and nonporous anode shrouds," *J. Nucl. Mater.*, vol. 444, no. 1–3, pp. 261–269, 2014, doi: 10.1016/j.jnucmat.2013.09.061.

[52] C. S. Seo, S. Bin Park, B. H. Park, K. J. Jung, S. W. Park, and S. H. Kim, "Electrochemical Study on the Reduction Mechanism of Uranium Oxide in a LiCl-Li2O Molten Salt," *J. Nucl. Sci. Technol.*, vol. 43, no. 5, pp. 587–595, 2006, doi: 10.1080/18811248.2006.9711137.

[53] H. Shin, J. Hur, S. M. Jeong, and K. Y. Jung, "Direct electrochemical reduction of titanium dioxide in molten lithium chloride," *J. Ind. Eng. Chem.*, vol. 18, no. 1, pp. 438–442, 2012, doi: 10.1016/j.jiec.2011.11.111.

[54] S. M. Jeong, H. S. Shin, S. S. Hong, J. M. Hur, J. B. Do, and H. S. Lee, "Electrochemical reduction behavior of U3O8 powder in a LiCl molten salt," *Electrochim. Acta*, vol. 55, no. 5, pp. 1749–1755, 2010, doi: 10.1016/j.electacta.2009.10.060.

[55] M. Iizuka, T. Inoue, M. Ougier, and J. Glatz, "Electrochemical Reduction of (U , Pu) O2 in Molten LiCl and CaCl 2 Electrolytes," *J. Nucl. Sci. Technol.*, vol. 44, no. 5, pp. 801–813, 2007, doi: 10.1080/18811248.2007.9711869.

[56] G. Qiu, K. Jiang, M. Ma, D. Wang, X. Jin, and G. Z. Chen, "Roles of cationic and elemental calcium in the electro-reduction of solid metal oxides in molten calcium chloride," *Zeitschrift fur Naturforsch. - Sect. A J. Phys. Sci.*, vol. 62, no. 5–6, pp. 292–302, 2007, doi: 10.1515/zna-2007-5-610.

[57] J. M. Hur, J. S. Cha, and E. Y. Choi, "Can carbon be an anode for electrochemical reduction in a LiCl-Li 2O molten salt?," *ECS Electrochem. Lett.*, vol. 3, no. 10, pp. 5–8, 2014, doi: 10.1149/2.0071410eel.

[58] C. Schwandt, "Understanding the electro-deoxidation of titanium dioxide to titanium metal

via the FFC-Cambridge process," vol. 122, no. 4, pp. 213–218, 2013, doi: 10.1179/0371955313Z.00000000071.

[59] G. Z. Chen and D. J. Fray, "Understanding the electro-reduction of metal oxides in molten salts," *TMS Light Met.*, no. March 2004, pp. 881–886, 2004.

[60] S. Wang, F. Zhang, X. Liu, and L. Zhang, "CaO solubility and activity coefficient in molten salts CaCl 2 – x," vol. 470, pp. 105–107, 2008, doi: 10.1016/j.tca.2008.02.007.

[61] E. Y. Choi *et al.*, "Reoxidation of uranium metal immersed in a Li2O-LiCl molten salt after electrolytic reduction of uranium oxide," *J. Nucl. Mater.*, vol. 485, pp. 90–97, 2017, doi: 10.1016/j.jnucmat.2016.12.017.